

Unconventional Superconductivity in the Vicinity of Strong First-Order Helimagnetic Transition in CrAs: ^{75}As -Nuclear Quadrupole Resonance Study

Hisashi Kotegawa¹, Hideki Tou¹, Hitoshi Sugawara¹, and Hisatomo Harima¹

¹*Department of Physics, Kobe University, Kobe 657-8501, Japan*

(Dated: December 6, 2024)

Pressure-induced superconductivity was recently discovered in binary helimagnet CrAs. We report the results of measurements of nuclear quadrupole resonance for CrAs under pressure. In the vicinity of the critical pressure, P_c , between the helimagnetic (HM) and paramagnetic (PM) phases, a phase separation is observed. The large internal field remaining in the phase-separated HM state indicates that the HM phase disappears through a strong first-order transition. The nuclear spin-lattice relaxation rate, $1/T_1$, reveals that substantial magnetic fluctuations are present in the PM state; however, the system is not close to a quantum criticality. The absence of a coherence effect in $1/T_1$ in the superconducting state provides evidence that CrAs is the first Cr-based unconventional superconductor.

PACS numbers: 74.25.nj 74.70.-b 75.30.Kz 74.20.Pq

In a conventional Bardeen-Cooper-Schrieffer (BCS) superconductor, electrons form Cooper pairs through negative interactions via an electron-phonon coupling. This gives a sign-uniform s -wave character to the superconducting (SC) gap symmetry. If positive interactions work electron pairs to induce superconductivity, unconventional superconductivity with a sign-changing order parameter is realized beyond the well established simple s -wave. This fascinating form of superconductivity has been discovered in specific materials, such as heavy fermion systems, high- T_c cuprates, organic systems, ruthenate, and recent Fe-based superconductors. A common feature of these materials is that superconductivity appears due to the instability of some degree of freedom, which is mainly induced on the verge of a magnetically ordered phase.

Very recently, Wu *et al.* and Kotegawa *et al.* independently discovered pressure-induced superconductivity in CrAs in the vicinity of the helimagnetic (HM) phase [1, 2]. This is the first example of superconductivity found in a Cr-based magnetic system. CrAs has a MnP-type orthorhombic crystal structure with a $Pnma$ space group. This structure possesses a space-inversion symmetry, but it is locally missing at the Cr and As sites, and both of these atoms form a zigzag chain along the a -axis. The magnetic transition of the first order into a double-helical state occurs at $T_N \sim 265$ K. This transition is accompanied by a large magnetostriction, and a lowering of the crystal structure symmetry has not been reported [3, 4]. The propagation vector is incommensurate with $0.354 \cdot 2\pi c^*$, where c^* is an unit vector along the c axis, and magnetic moments of $\sim 1.7\mu_B/\text{Cr}$ lie in the ab plane [5, 6]. The application of pressure drastically suppresses T_N , and the HM phase disappears above a critical pressure of $P_c \sim 0.7$ GPa [1, 2, 7]. Superconductivity appears together with the suppression of the HM phase, showing a maximum SC transition temperature of $T_c \sim 2.2$ K at ~ 1.0 GPa, after which T_c decreases gradually with increasing pressure. The pressure-temperature phase diagram of CrAs with first-order magnetic tran-

sition is reminiscent of those of some pressure-induced Fe-based superconductors, such as SrFe_2As_2 [8, 9]. Magnetic interactions are conjectured to play a crucial role in the induction of superconductivity in CrAs. Experimental investigation is desired to elucidate how SC symmetry is realized in CrAs.

Here, we report the results of nuclear quadrupole resonance (NQR) measurements under ambient and high pressures to elucidate the underlying electronic correlations and SC symmetry in CrAs. From the nuclear spin relaxation rate, $1/T_1$, we obtained a strong suggestion that the superconductivity realized under moderate magnetic fluctuations of CrAs is of unconventional nature.

Single crystals of CrAs were prepared by the Sn-flux method from a mixture of Cr:As:Sn=1:1:10 as described in Ref. [2]. The NQR measurements under pressure were performed using a piston-cylinder cell and Daphne 7474 as the pressure-transmitting medium [10]. The applied pressure was estimated from the T_c of the lead manometer. Several as-grown single crystals were put into the pressure cell, and NQR measurements were performed using the conventional spin-echo method for the ^{75}As nucleus. ^3He cryostat was utilized to perform NQR measurement at low temperatures. To obtain T_1 in the paramagnetic (PM) state, the recovery curves obtained at the $(\pm 1/2 \leftrightarrow \pm 3/2)$ transition are fitted by a single exponential function. Calculations of band structure and electric field gradient (EFG) were obtained through a full-potential LAPW (linear augmented plane wave) calculation within the LDA (local density approximation).

Figure 1 shows the ^{75}As NQR- or the so-called zero-field nuclear magnetic resonance (NMR)-spectra in the HM state at ambient pressure, where the energy levels of the nuclear spins are mainly lifted by the internal field. Because the nuclear spin of ^{75}As is $I = 3/2$, and because all the As sites in the crystal are equivalent to each other, three transitions were expected for a commensurate magnetic structure, whereas complicated spectra composed of six peaks were obtained at both 5 and 100 K. Each peak being not well separated suggests the presence of a spatial

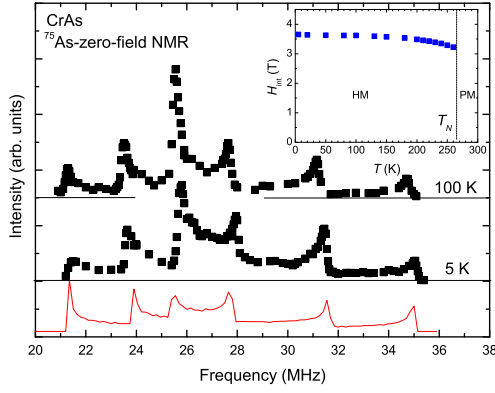


FIG. 1: (color online) Zero-field NMR spectra for the ^{75}As nucleus at ambient pressure. The complicated spectrum at 5 K can be reproduced by a model based on the HM state reported by previous neutron scattering measurements, as shown by the red curve. The spectral shape is independent of temperature. The inset shows the temperature dependence of H_{int} at the As site, which decreased gradually with increasing temperature and remained large at T_N due to the first-order transition.

modulation of the internal field at the As sites. In fact, previous neutron scattering measurements have shown that the magnetic structure is incommensurate with the propagation vector of $0.354 \cdot 2\pi c^*$ [5, 6]. Because the measurements also showed that the magnetic moments lay in the ab plane, we performed a simulation based on this magnetic structure; that is, we assumed that the internal field, H_{int} , at the As site was distributed in the ab plane through dominant isotropic hyperfine coupling between the Cr-moments and the As nuclei. The EFG parameter at the As site in the HM state is unknown; however, crystallographically one of the principal axes is restricted to be along the b -axis. We obtained the red curve to reproduce the experimental result, which gave the quadrupole frequency as $\nu_Q = 15.8$ MHz, and the asymmetry parameter as $\eta = 0.95$, and $H_{int}^a = 3.82$ T along the a -axis, and $H_{int}^b = 3.35$ T along the b -axis. The direction of the maximum principal axis of the EFG, V_{zz} , was tilted from a -axis towards the c -axis at 29.8° . There was good agreement between the simulation and the experimental results, supporting the validity of the results from the neutron scattering measurements [5, 6]. The anisotropy of H_{int} in the ab plane is considered to originate in the small anisotropy of the hyperfine coupling constant. The inset shows the temperature dependence of $H_{int} = (H_{int}^a + H_{int}^b)/2$. It decreases gradually with increasing temperature and vanishes suddenly at T_N because of a first-order phase transition.

Figure 2 shows the pressure dependence of zero-field NMR and NQR spectra measured at 5 K. The spectrum is remarkably broadened under pressure, probably owing to a distribution of the EFG, but the spectral shape remains similar. There is no signature of a change in the magnetic structure under pressure, meaning that super-

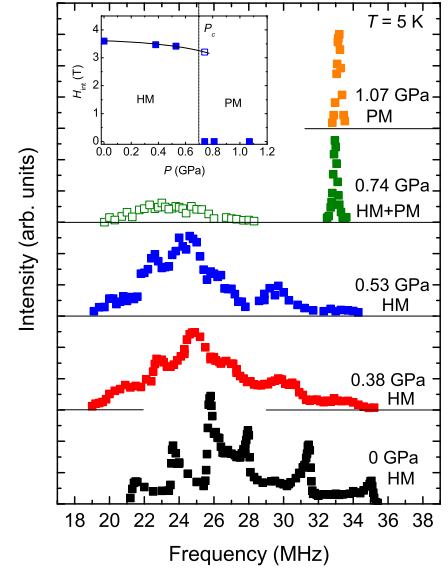


FIG. 2: (color online) Pressure dependence of spectra at 5 K. The spectrum is broadened by applying pressure, but its structure is similar up to 0.53 GPa. At 0.74 GPa close to P_c , the signal from the HM phase is suppressed and the new signal corresponding to the PM phase appears, indicating that the phase separation between the HM and PM phases occurs in the vicinity of P_c . The intensity of the HM phase at 0.74 GPa is ~ 5 times smaller than that at 0.53 GPa. The inset shows the pressure dependence of H_{int} , which has a large value on the border of the HM-PM transition as well as the case of the temperature dependence shown in the inset of Fig. 1. The dotted line represents P_c , as determined by resistivity measurement [2].

conductivity occurs adjacent to the incommensurate HM state. The overall spectrum moves to the low-frequency side with increasing pressure due to a reduction of H_{int} . At 0.74 GPa, the intensity of the HM state is drastically suppressed, whereas another sharp spectrum corresponding to the PM state appears at ~ 33 MHz, which is the $(\pm 1/2 \leftrightarrow \pm 3/2)$ transition. We cannot deduce the η in the PM state experimentally from this resonance frequency, but our first-principal calculation using a structural parameter at ambient pressure and room temperature gave $\nu_Q = 23.7$ MHz and $\eta = 0.73$ in the PM state, where V_{zz} lies along the direction tilted from the c -axis towards the a -axis at 35.5° . By adopting $\eta = 0.73$, we obtained $\nu_Q = 30.4$ MHz, which was not so far from the calculation. We observed simultaneously the spectra for both the HM and PM states at 0.74 GPa, giving microscopic evidence of a phase separation. We did not observe the signal from the HM state at 0.81 GPa; thus, the homogeneous PM phase was realized above approximately 0.8 GPa. The inset shows the pressure dependence of H_{int} , which gradually decreases under pressure and maintains a large value even in the vicinity of P_c . These facts indicate that the HM-PM transition at low temperatures is of strong first-order. Our observations suggest that CrAs does not possess a quantum critical

point (QCP) on the pressure-temperature phase diagram. The moderate pressure dependence of H_{int} indicates that the HM interactions are insensitive to pressure irrespective of strong suppression of T_N [1, 2, 7]. Thus, the suppression of T_N is suggested to be induced crucially by a suppression of magnetostriction, which corresponds with an increase in volume of $\sim 4\%$ below T_N at ambient pressure [3, 4].

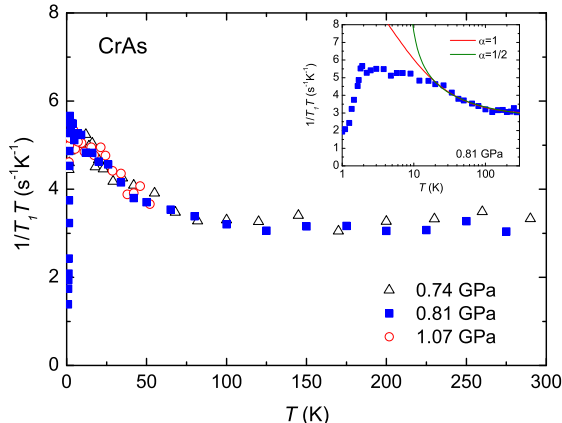


FIG. 3: (color online) Temperature dependence of $1/T_1T$ in the PM state, where superconductivity occurs. The increase in $1/T_1T$ toward low temperatures demonstrates the development of magnetic fluctuations. The inset shows the same data at 0.81 GPa in a logarithmic scale. $1/T_1T$ does not obey Curie-Weiss-like behavior down to T_c and is suppressed below ~ 20 K.

Figure 3 shows the temperature dependence of $1/T_1T$ in the PM phase under pressure. $1/T_1T$ is almost constant for temperatures from 300 to 100 K, and increases toward lower temperatures below ~ 100 K. The deviation from Fermi liquid behavior of $T_1T = \text{const.}$ below ~ 100 K clearly demonstrates the presence of magnetic correlations developing toward lower temperatures. Similar behaviors in $1/T_1T$ have been observed in other d -electron superconductors adjoining magnetic phases such as cobalt oxyhydrate [11–13] and many Fe-based superconductors [9, 14–17]. In such itinerant magnetic systems, $1/T_1T$ is generally composed of two contributions as follows.

$$\frac{1}{T_1T} = \frac{A}{(T + \theta)^\alpha} + B \quad (1)$$

Here, A and B are temperature-independent constants. The first term is given by spin correlations developing at a specific wave vector. In a self-consistent renormalization theory [18], the 3D ferromagnetic and 2D antiferromagnetic correlations give $\alpha = 1$, and the 3D antiferromagnetic case gives $\alpha = 1/2$. $\theta = 0$ means that the system is located at a QCP. The second term is obtained from a uniform susceptibility and from a relaxation through orbital angular momentum, which are both related to the density of states (DOS) at the Fermi level and are independent of temperature in typical metals. In cobalt

oxyhydrate [12, 13] and some Fe-based superconductors [14, 16, 17], low θ s close to zero are obtained, suggesting that these systems are located in the vicinity of the quantum criticality. We attempted to fit $1/T_1T$ for CrAs to this form but could not reproduce the data down to T_c because of a suppression of $1/T_1T$ below ~ 20 K. As shown in the inset in a logarithmic scale, the increase in $1/T_1T$ toward low temperatures is suppressed below ~ 20 K, and $1/T_1T$ approaches a constant value at low temperatures. We measured $1/T_1T$ from 0.74 to 1.07 GPa, but differences were small in this pressure range. From the fitting in a temperature range of 20 – 300 K, we obtain $\theta = 4.6$ K for $\alpha = 1$ and $\theta = -7.6$ K for $\alpha = 1/2$, although α was not determined from the fitting. The negative or low θ suggest that CrAs has magnetic correlations developing toward magnetic ordering at high temperatures above ~ 20 K, but which are suppressed at low temperatures. $1/T_1T$ is very close to constant in a narrow temperature range just above T_c , which is consistent with an observation of $\rho \sim T^2$ behavior in a narrow temperature window in resistivity measurement [2]. If we fit $1/T_1T$ between T_c and 20 K to the above form, we obtain $\theta = 58$ K for $\alpha = 1$ and $\theta = 41$ K for $\alpha = 1/2$. These high θ s indicate that CrAs is not close to a QCP, even in the vicinity of P_c . Note that the suppression of the magnetic fluctuations below ~ 20 K is observed even in the PM state at 0.74 GPa, where the phase separation occurs. This is in sharp contrast to some Fe-based superconductors, in which the quantum critical behavior, i.e., $\theta \sim 0$, has been observed [16, 17]. In addition to the pressure dependence of H_{int} , $1/T_1T$ also suggests that a QCP is absent in CrAs under pressure.

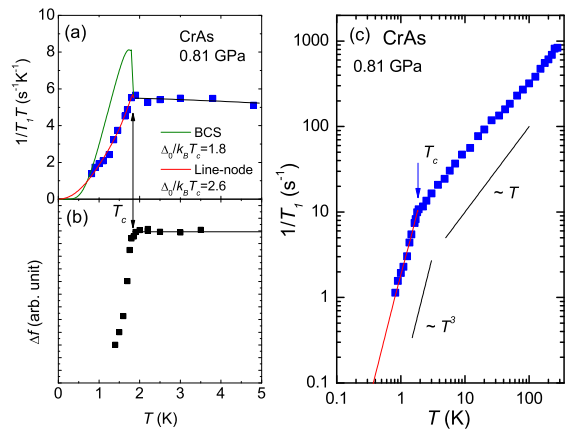


FIG. 4: (color online) (a) Temperature dependence of $1/T_1T$ below 5 K measured under a zero field. The clear reduction in $1/T_1T$ is observed below $T_c = 1.85$ K, which is determined by the ac-susceptibility shown in Fig. 4 (b). The green curve indicates a calculation based on a conventional BCS, whereas the red curve indicate one based on a line-node model (polar-type). $1/T_1T$ is clearly reproduced by the unconventional model. (c) Temperature dependence of $1/T_1$ at 0.81 GPa. The red curve based on the line-node model is also plotted. The temperature dependence of $1/T_1$ is close to T^3 below T_c .

Now, we discuss $1/T_1$ in the SC state. Figure 4(a) shows the temperature dependence of $1/T_1T$ below 5 K measured at 0.81 GPa. The temperature dependence of ac susceptibility measured by an *in-situ* NMR coil is also shown in Fig. 4(b). It clearly shows a diamagnetic signal below $T_c = 1.85$ K. This T_c is slightly lower than zero resistance, which appears below ~ 2.1 K at a similar pressure [2]; however, the clear SC transition in the susceptibility obtained for several crystals in the pressure cell ensures that the T_c is quite homogeneous among the different crystals. Below T_c , $1/T_1T$ shows a clear reduction without the signature of a coherence peak (Hebel-Slichter peak), which is a marker of a BCS superconductor [19]. The green curve in the figure indicates calculated $1/T_1T$ for a conventional BCS model, which has an isotropic gap of $\Delta_0/k_B T_c = 1.8$. Evidently this does not match the experimental result below T_c . On the other hand, the red curve indicates calculated $1/T_1T$ for a line-node model (polar-type) with $\Delta_0/k_B T_c = 2.6$, and reproduce the data well, meaning that the coherence effect is completely absent in CrAs, and suggesting strongly that superconductivity is not of the conventional BCS but unconventional in nature. CrAs is the first example of unconventional superconductivity seen in Cr-based systems.

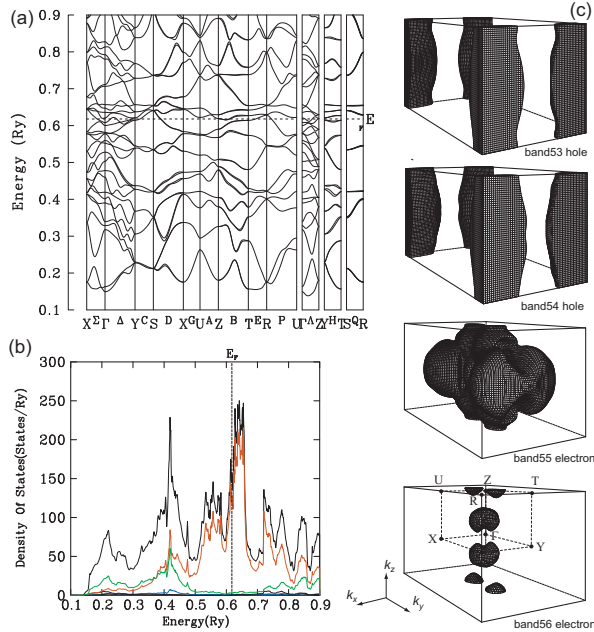


FIG. 5: (color online) (a) Band dispersion, (b) DOS, and (c) Fermi surfaces of CrAs calculated in the PM state. The calculation was performed using the structural parameter at ambient pressure and room temperature [6]. In Fig. (b), the red, green and blue curves indicate the partial DOS from Cr-*d*, As-*p*, and Cr-*p* orbitals, respectively.

Here, we used a polar-type line-node model as a simple

example, which gives T^3 dependence in $1/T_1$ at low temperatures, but the SC gap function is not restricted by the present experiment. Experiences in Fe-based superconductors show us that careful measurements and analyses are required in T_1 to determine the SC gap structure in the case of multi-gap superconductors. For example, sign-changing nodeless s^\pm -wave symmetry is considered to be realized in some of Fe-based superconductors, and this symmetry can reproduce the T^3 dependence of $1/T_1$ [20–22]. In fact, our band calculation, shown in Figs. 5(a–c), suggests that the Fermi surface of CrAs, which is formed mainly by the Cr-*d* orbitals, is composed of several sheets. The DOS shown in Fig. 5(b), which is almost consistent with a previous report [23], indicates that the peak DOS is located just above the Fermi energy, E_F . As shown in Fig. 5(c), the electron Fermi surfaces have 3D character, whereas the hole surfaces are 2D-like and are almost degenerated. The present NQR results strongly suggest that a sign in the SC gap must change somewhere in the momentum space; however, the possibility of a nodeless gap cannot be excluded. We are planning to measure $1/T_1$ at lower temperatures in future research to investigate the details of the SC gap structure in CrAs. It is also an important issue to investigate how magnetic fluctuation develops in this system. To clarify the character of magnetic fluctuations, inelastic neutron scattering measurements and NMR measurements under different magnetic field directions are essential.

In summary, we performed NQR measurements on pressure-induced superconductor CrAs. The phase separation between the HM and PM phases in the vicinity of P_c and the insensitivity of H_{int} against pressure provide microscopic evidence of strong first-order HM-PM transition at P_c . $1/T_1T$ shows a Curie-Weiss-like behavior from 100 K to ~ 20 K, suggesting that substantial magnetic fluctuations remain in the PM phase, irrespective of the strong first-order magnetic transition. However, these fluctuations are suppressed gradually below ~ 20 K, resulting in the absence of a QCP in this system. $1/T_1T$ does not show a coherence peak, but decreases sharply below T_c , giving a clear indication that superconductivity in CrAs is of an unconventional nature. This first example of unconventional superconductivity in a Cr-based system opens a new route to the development of the field of superconductivity.

Acknowledgements

We thank Haruki Matsuno for the experimental support. This work has been supported in part by Grants-in-Aid for Scientific Research (Nos. 22740231, 20102005, and 24340085) from the Ministry of Education, Culture, Sports, Science and Technology (MEXT) of Japan.

-
- [1] W. Wu, J. Cheng, K. Matsubayashi, P. Kong, F. Lin, C. Jin, N. Wang, Y. Uwatoko, and J. Luo, arXiv:1406.6431.
 - [2] H. Kotegawa, S. Nakahara, H. Tou, and H. Sugawara, J. Phys. Soc. Jpn. **83**, 093702 (2014).
 - [3] H. Boller and A. Kallelt, Solid State Comuni. **9**, 1699 (1971).
 - [4] T. Suzuki and H. Ido, J. Appl. Phys. **73**, 5686 (1993).
 - [5] H. Watanabe, N. Kazama, Y. Yamaguchi, and M. Ohashi, J. Appl. Phys. **40**, 1128 (1969).
 - [6] K. Selte, A. Kjekshus, W. E. Jamison, A. Andresen, and J. E. Engebretsen, Acta Chem. Scand. **25**, 1703 (1971).
 - [7] É. A. Zavadskil and I. A. Sibarova, Sov. Phys. JETP **51**, 542 (1980).
 - [8] H. Kotegawa, H. Sugawara, and H. Tou: J. Phys. Soc. Jpn. **78**, 013709 (2009).
 - [9] K. Kitagawa, N. Katayama, H. Gotou, T. Yagi, K. Ohgushi, T. Matsumoto, Y. Uwatoko, and M. Takigawa, Phys. Rev. Lett. **103**, 257002 (2009).
 - [10] K. Murata, K. Yokogawa, H. Yoshino, S. Klotz, P. Munsch, A. Irizawa, M. Nishiyama, K. Iizuka, T. Nanba, T. Okada, Y. Shiraga, and S. Aoyama: Rev. Sci. Instrum. **79**, 085101 (2008).
 - [11] T. Fujimoto, G. -q. Zheng, Y. Kitaoka, R. L. Meng, J. Cmaidalka, and C.W. Chu, Phys. Rev. Lett. **92**, 047004 (2004).
 - [12] Y. Ihara, H. Takeya, K. Ishida, C. Michioka, K. Yoshimura, K. Takada, T. Sasaki, H. Sakurai, and E. Takayama-Muromachi, Phys. Rev. B **75**, 212506 (2007).
 - [13] E. Kusano, S. Kawasaki, K. Matano, G.-q. Zheng, R. L. Meng, J. Cmaidalka, and C. W. Chu, Phys. Rev. B **76**, 100506(R) (2007).
 - [14] H. Fukazawa, T. Yamazaki, K. Kondo, Y. Kohori, N. Takeshita, P. M. Shirage, K. Kihou, K. Miyazawa, H. Kito, H. Eisaki, and A. Iyo, J. Phys. Soc. Jpn. **78**, 033704 (2009).
 - [15] T. Imai, K. Ahilan, F. L. Ning, T. M. McQueen, and R. J. Cava, Phys. Rev. Lett. **102**, 177005 (2009).
 - [16] Y. Nakai, T. Iye, S. Kitagawa, K. Ishida, H. Ikeda, S. Kasahara, H. Shishido, T. Shibauchi, Y. Matsuda, and T. Terashima, Phys. Rev. Lett. **105**, 107003 (2010).
 - [17] T. Oka, Z. Li, S. Kawasaki, G. F. Chen, N. L. Wang, and G. -q. Zheng, Phys. Rev. Lett. **108**, 047001 (2012).
 - [18] T. Moriya, J. Mag. Mag. Mat. **100**, 261 (1991).
 - [19] L. C. Hebel and C. P. Slichter, Phys. Rev. **113**, 1504 (1959).
 - [20] D. Parker, O. V. Dolgov, M. M. Korshunov, A. A. Golubov, and I. I. Mazin: Phys. Rev. B **78**, 134524 (2008).
 - [21] A. V. Chubukov, D. Efremov, and I. Eremin, Phys. Rev. B **78**, 134512 (2008).
 - [22] Y. Nagai, N. Hayashi, N. Nakai, H. Nakamura, M. Okumura, and M. Machida: New J. Phys. **10**, 103026 (2008).
 - [23] T. Ito, H. Ido, and K. Motizaki, J. Mag. Mag. Mat. **310**, e558 (2007).